Submitted to the 29th International Conference on High-Energy Physics ICHEP98,
Vancouver, Canada, July 1998

Transverse Energy Production in Deep-Inelastic Scattering at HERA

H1 Collaboration

Abstract

Measurements of transverse energy flow are presented for deep-inelastic scattering events produced in positron-proton collisions at HERA. The kinematic range covers squared momentum transfers (Q^2) from 2.5 GeV^2 to $40\,000$ GeV^2 and x, the Bjorken scaling variable, down to $3 \cdot 10^{-5}$. The transverse energy flow is measured in the hadronic centre-of-mass frame and is studied as a function of Q^2, x and pseudorapidity (in the range $-3 < \eta^* < 5.5$). A comparison is made with QCD-based Monte Carlo models. The behaviour of the mean transverse energy in a central pseudorapidity range, $-0.5 < \eta^* < 0.5$, and a photon fragmentation interval, defined to lie in the range $2.0 < \eta^* < 3.0$, is studied as a function of Q^2 and as a function of the invariant mass W of the hadronic final state.

Abstract: 553
Parallel sessions: 5,3
Plenary sessions: 7,5

1 Introduction

The transverse energy flow (E_T flow) in deep-inelastic lepton nucleon scattering contains important information about the hadronic final state. It is sensitive to both perturbative QCD (pQCD) and fragmentation processes and has already proven to be an important discriminant for Monte Carlo models [1]. A detailed knowledge of the transverse energy is therefore helpful in testing and improving the different models.

Although the Monte Carlo treatment of DIS is traditionally based on the picture of a point-like photon probing the hadronic structure of the proton, one can also try to understand electron-proton scattering by assuming the exchanged photon acts as a hadronic object. In such a VMD[1]-like picture the photon fluctuates into a hadron which then scatters off the proton. This approach is expected to be valid at low Q^2 but can be extended to the high Q^2 region [2–4]. In the proton rest frame the fluctuation length [3]

$$l = \frac{2\nu}{m^2 + Q^2} = \frac{1}{m_P x(1 + m^2/Q^2)} \tag{1}$$

gives the typical distance travelled by a vacuum fluctuation of mass m. At low Q^2 the photon may fluctuate into e.g. a ρ meson ($m = m_\rho$) giving $l \approx 2\nu/m_\rho^2$. At high Q^2 ($Q^2 >> m^2$) we have $l \approx 1/(xm_p)$, where m_p is the mass of the proton. In general the photon may fluctuate into any of the final states observed in e^+e^- annihilations. If the fluctuation length is large compared to the typical interaction length of the strong force the photon will behave like a hadronic object. Therfore electron-proton interactions are expected to resemble hadron-hadron scattering not only in photoproduction ($Q^2 \approx 0$) but also at higher values of Q^2 when x is sufficiently small.

The large amount of data collected by H1 over recent years now allows an investigation of energy flow over a considerably extended kinematic range, particularly at high Q^2 ($Q^2 > 100$ GeV^2) where a far more detailed measurement is now possible than previously reported [5]. On the other hand, it turns out that the transverse energy flow is more sensitive to systematic effects at high Q^2, compared to the low Q^2 domain. In order to benefit from the advantage in statistics it is therefore necessary to improve our understanding of systematic effects.

In the following the high Q^2 results are based on data (8.2 pb^{-1}) taken in 1996 with the H1 detector at HERA. The low Q^2 results are based on 1994 data (2.7 pb^{-1}) that have been partly presented elsewhere [6] but cover now an extended range in η^* towards the proton remnant [7].

2 Detector Description

The LAr calorimeter is the main part of the H1 detector for this measurement. It covers a polar angle Θ from 4° to 154° (with respect to the proton direction), and it is used to measure the particles of the hadronic final state and, for high Q^2 events, the scattered positron. At low Q^2 the backward electromagnetic calorimeter (BEMC) extends the Θ range for the scattered positron up to 176°. A backward proportional chamber (BPC), situated in front of the BEMC, serves to measure the impact point of the scattered positron. The transverse energy flow measurement is extended in proton direction with a small calorimeter (PLUG) with copper absorber and silicon

[1]Vector Meson Dominance

pad readout, covering the region between the beam-pipe and the LAr cyrostat ($0.7^\circ < \Theta < 3.3^\circ$). For the high Q^2 region the additional information about the direction of the scattered positron supplied by the central trackers is crucial to control systematic effects.

See [8] for more details about the H1 detector.

3 Event Selection

In this analysis two independent event samples are considered from the 1994 and the 1996 data taking periods respectively. The 1994 low Q^2 sample consists of events in which the scattered positron is found in the BEMC. The Q^2 values of this sample lie in the range 2.5 GeV^2 $< Q^2 <$ 100 GeV^2. In order to reach Q^2 values of less than 10 GeV^2 a dedicated run period (58 nb^{-1}) is included in which the nominal vertex position is shifted by about 67 cm in the proton direction. The high Q^2 sample consists of events collected in 1996. For this sample, the scattered positron is found in the LAr calorimeter and Q^2 is required to be larger than 100 GeV^2.

DIS events are selected by demanding a well-reconstructed scattered positron with an energy larger than 12 GeV. The event kinematics are determined using the scattered positron energy E'_e and polar angle Θ_e (electron method). The kinematic plane is divided into several slices in x and Q^2. The bin sizes are adapted to the experimental resolution to keep migration effects small. In addition the following selection criteria are applied:

- There has to be a reconstructed event vertex within ± 30 cm of the mean z-position of the vertex.
- The longitudinal momentum balance has to be within 30 GeV $< \sum_i E_i - P_{zi} <$ 70 GeV, where the sum runs over all energy depositions in the LAr and the backward calorimeter including the scattered positron.
- W^2, the invariant mass squared of the hadronic final state, can be determined from the scattered positron (W_e^2) or from energy clusters in the calorimeter (W_h^2). Both W_e^2 and W_h^2 are required to be larger than $4\,400$ GeV^2.
- $y_e < 0.6$, where $y_e = 1 - E'_e/E_e \sin^2 \Theta_e/2$ and E_e is the energy of the incoming positron. (The requirement $W_e^2 > 4\,400$ GeV^2 is approximately equivalent to $y_e > 0.05$)

For the low Q^2 sample the positron candidate is required to be found within the angular acceptance of the BEMC ($157^\circ < \Theta_e < 173^\circ$ and $164^\circ < \Theta_e < 176^\circ$ for the shifted vertex data). In addition, electron identification cuts to suppress photoproduction background are made using the information obtained from the BEMC cluster radius and the matching of the cluster with a charged particle signal in the BPC. After these cuts the remaining photoproduction background is estimated to be less than 3 %.

For the high Q^2 sample the scattered positron candidate is required to be found within the LAr calorimeter ($\Theta_e > 150^\circ$). Since the high Q^2 analysis is especially sensitive to QED radiative effects (see 4.2) further selection criteria are included:

- $0.5 < y_h/y_e < 1.3$. The variable y_h is given by the Jacquet Blondel method [9]: $y_h = \frac{1}{2}\Sigma/E_e$ where $\Sigma = \sum_i (E_i - p_{zi})$ and i refers to all energy clusters detected in the calorimeters except the scattered positron.

- In addition to the electron method, the Σ method [10] is also used to calculate x and Q^2 and a requirement is made that both methods should prescribe the same kinematic bin for a given event. According to the Σ method Q^2, y and x are given by (Σ as above) $Q^2_\Sigma = E'_e \sin^2\Theta_e/(1-y_\Sigma)$, $y_\Sigma = \Sigma/(\Sigma + E'_e(1-\cos\Theta_e))$ and $x_\Sigma = Q^2_\Sigma/(sy_\Sigma)$

Both conditions are designed to remove events suffering from strong QED initial state radiation or with a badly reconstructed positron. Since they have a more complicated structure, careful studies have been performed to prove that these cuts do not introduce any bias to our results.

We have also analysed high Q^2 data from 1994 and the transverse energy flow measurements are consistent within their statistical errors. Because of the different correction procedure for the 1994 and the 1996 data sample and significantly better statistics of the 1996 high Q^2 sample we have not combined the two measurements and present for the high Q^2 region only results based on 1996 data.

4 Transverse Energy Flow

The E_T flow , i.e. $\langle E_T \rangle$ versus pseudorapidity η^*, is presented in the hadronic centre-of-mass system (hCMS), the centre-of-mass system of the proton and the exchanged boson. While in the laboratory frame (LAB) a sizeable contribution to the transverse energy is produced by the trivial kinematic recoil from the scattered lepton, in the hCMS transverse energy is due largely to perturbative QCD effects and fragmentation. The Lorentz transformation from the LAB into the hCMS therefore serves to isolate the physically interesting part of the E_T flow. The orientation of the axes has been chosen such that the proton direction defines the negative z axis. The data are corrected bin-by-bin for QED radiation and detector effects using the DJANGO event generator [11] and a full simulation of the H1 detector. The applied correction never exceeds 50%.

4.1 Transverse Energy Flow at Low Q^2

In addition to the selection criteria outlined in section 3 a further cut on the total energy produced in the angular region $4.4^\circ < \Theta < 15^\circ$ is imposed. The energy in this angular region is required to be larger than 0.5 GeV (E_{fwd} cut). This condition was introduced for the low Q^2 analysis in order to suppress so-called *rapidity-gap* events. It allows a comparison with Monte Carlo programs and pQCD calculations which is less dependent on uncertainties introduced by the attempt to model diffractive processes.

We present in Fig. 1 the E_T flow in 17 regions in x and Q^2 and compare them to 3 standard Monte Carlo models: ARIADNE [12], HERWIG [13] and LEPTO[2] [14]. The $\langle Q^2 \rangle$ covers a range from 3.2 GeV^2 to 70.2 GeV^2 and the $\langle x \rangle$ a range from $0.08 \cdot 10^{-3}$ to $7 \cdot 10^{-3}$. At low Q^2 the transverse energy flow is less sensitive to systematic effects than it is in the high Q^2 region (see 4.2). The systematic errors are not yet included in Fig. 1 but are estimated to be of the order of 10%. The two most forward data points in each $x - Q^2$ bin, i.e. the lowest points

[2] Throughout this paper default settings are used. Thus, the SCI (Soft Colour Interaction) model is included in all LEPTO predictions.

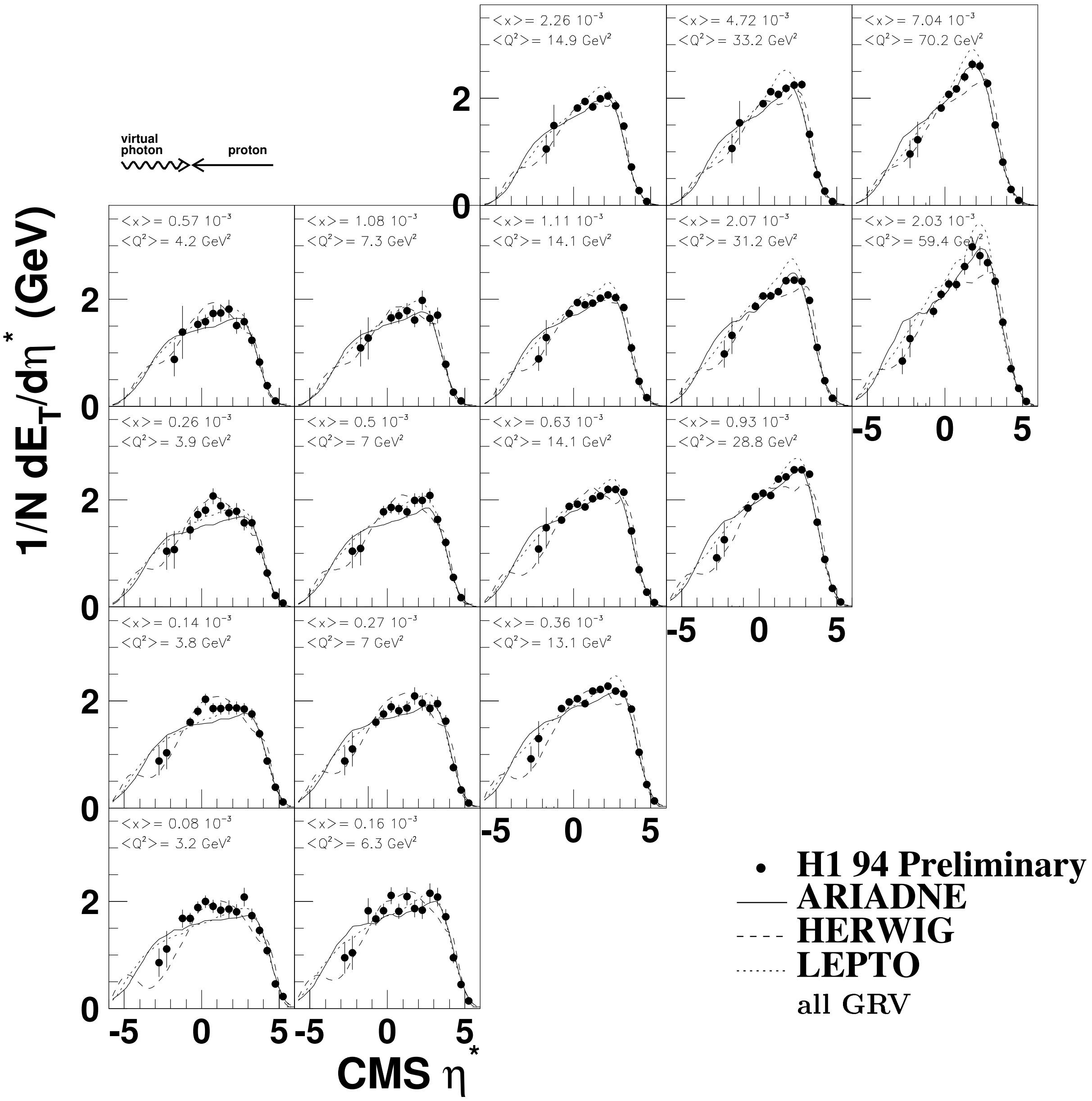

Figure 1: H1 preliminary results on the E_T flow at low Q^2 in the hCMS. The data are compared to 3 MC generators: ARIADNE 4.08, HERWIG 5.8 and LEPTO 6.4. The structure functions used are based on the GRV parametrizations [15]. Statistical errors are included for all data points. The lowest two data points in each x-Q^2 bin are measured with the PLUG calorimeter. For these data points statistical and systematic errors are added in quadrature.

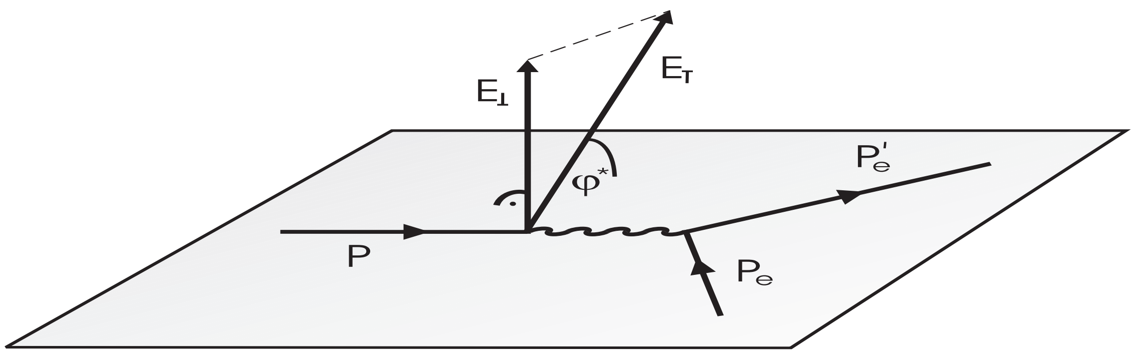

Figure 2: $E_\perp$ is the component of the transverse energy E_T perpendicular to the scattering plane. The scattering plane is defined by the incoming Proton P and the scattered positron P'_e. P_e is the incoming positron.

in η^*, have been measured with the PLUG calorimeter. Here systematic errors are included. The calibration procedure for the PLUG is less precise than for the other calorimeters resulting in a larger systematic error. This is mainly due to the large amount of dead material in front of the device [7].

The data exhibit a mean transverse energy of approximately 2 GeV per unit of rapidity. The E_T flow is plateau-like at low Q^2 (below ≈ 10 GeV^2) and becomes more peaked in the current region, $\eta^* > 0$, at larger Q^2. In the vicinity of the proton, i.e. at the smallest accessible pseudorapidity values, the production of transverse energy is suppressed. The Monte Carlo models give a good overall description of the measured E_T flow. Larger differences are found at $\eta^* < -1$ but our measurements do not prefer any of the Monte Carlo models due to the larger errors in the extreme forward region. Differences between the Monte Carlo models also appear at higher Q^2 and positive η^*. In this region LEPTO slightly overshoots the data. This difference is more pronounced in the high Q^2 sample.

4.2 Transverse Energy Flow at High Q^2

At high Q^2 the Lorentz transformation from the LAB to the hCMS requires great care. Any deviation from the true transformation produces an artificial contribution to the transverse energy seen in the hCMS. This is a more severe problem at high Q^2 since $\langle E_T \rangle$ increases with Q in the LAB but not in the hCMS. For this analysis the maximum $\langle E_T \rangle$ in the LAB is typically an order of magnitude larger than the $\langle E_T \rangle$ in the hCMS (about 20 GeV compared to 2 GeV). In practice the transformation is calculated from the energy and direction of the scattered positron, and there are several sources of bias: energy resolution, calibration and QED radiation. Although energy resolution and calibration of the H1 LAr calorimeter are well understood and the influence of QED radiation is well described by DJANGO, they remain an important source of systematic uncertainties. A change in the calculation of E_T was therefore necessary. For a particle with energy E and angle Θ with respect to the incoming proton, the transverse component is defined by $E_T = E \sin\Theta$. A deviation in the energy measurement of the scattered positron will result in an artificial component to the momentum of any particle in the hCMS. This component lies within the scattering plane[3] defined by the incoming proton and the scat-

[3]The H1 central tracker provides accurate information about the direction of the scattered positron. In addition QED radiation is, in almost all cases, collinear with the incoming or outgoing positron and does not change the direction of the scattered positron. Therefore, a better determination of the angle of the scattered positron is obtained than of its energy.

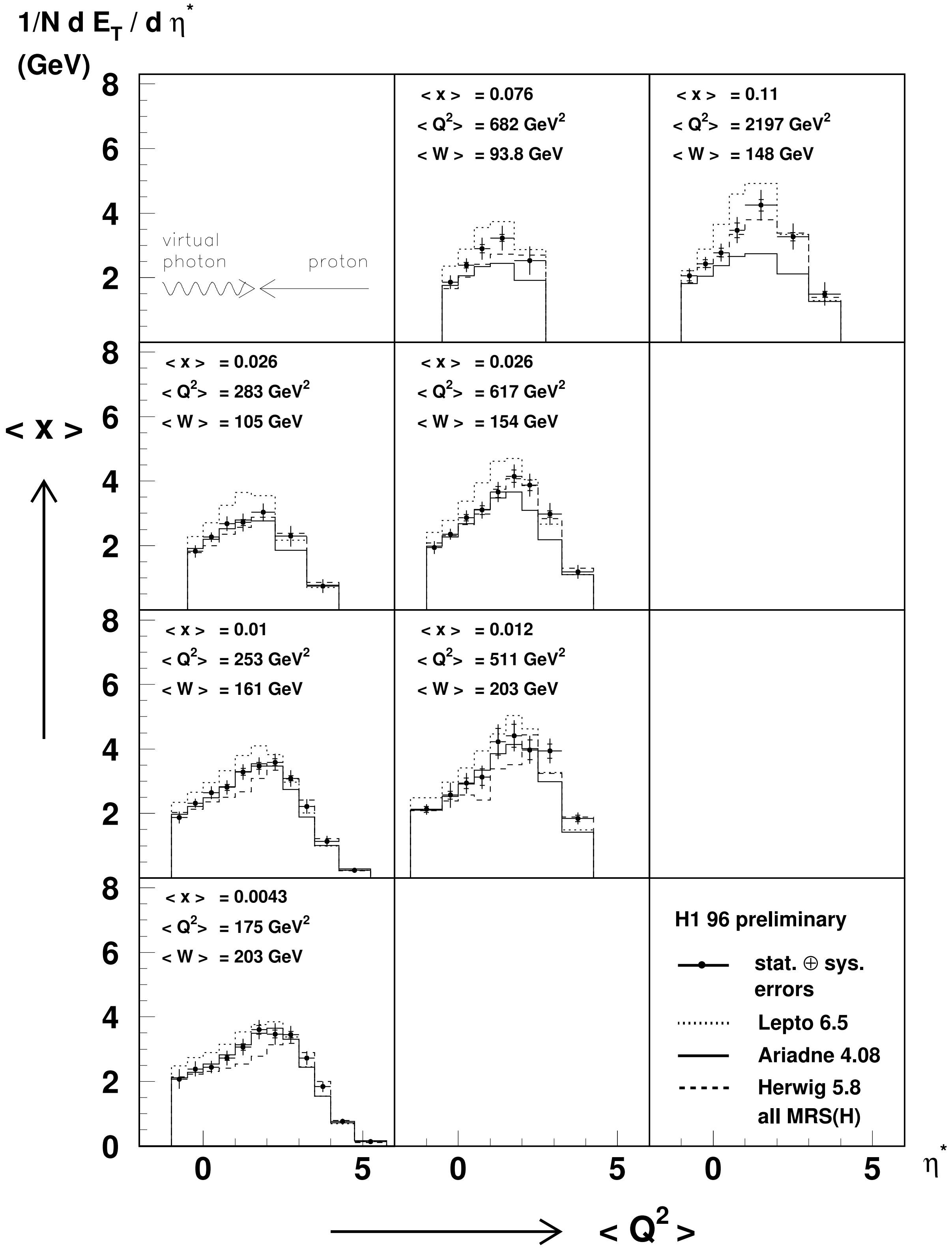

Figure 3: H1 preliminary results on the E_T flow in the hCMS at high Q^2. Systematic and statistical errors are added in quadrature. The data is compared to 3 MC generators: ARIADNE 4.08, HERWIG 5.8 and LEPTO 6.5. The structure functions used are based on the MRS(H) parametrizations [16].

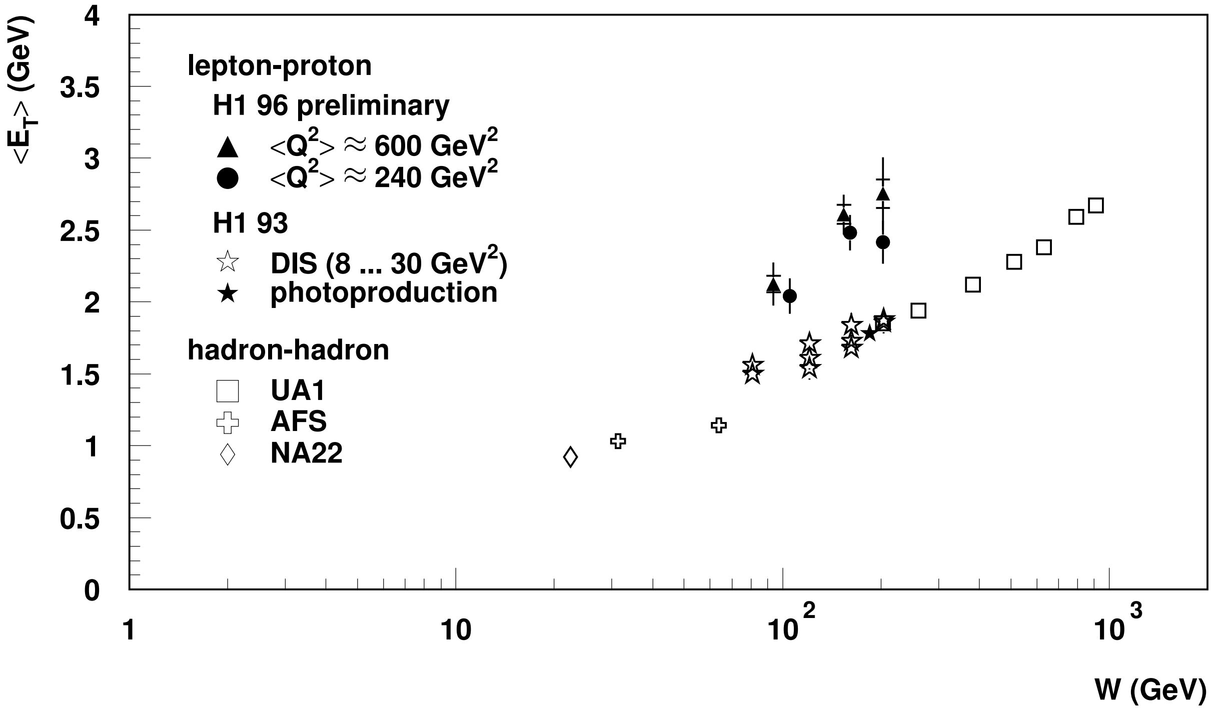

Figure 4: H1 preliminary results on the mean E_T in the central rapidity bin at high Q^2 as a function of W. The new data are combined with earlier H1 results at lower Q^2 including photoproduction data [5] and are compared to hadron-hadron results [17] ($p\bar{p}$ for UA1; pp for NA22 and AFS).

tered positron, as can be seen in Fig. 2. One can avoid this artificial momentum if only the component perpendicular to the scattering plane is taken into account. This component is given by

$$E_{\perp} = E_T |\sin \varphi^*| \frac{\pi}{2}. \tag{2}$$

Integrated over φ^* this is again equal to E_T, given an isotropic distribution of the transverse energy around the proton. In general φ^* asymmetries are expected but detailed MC studies show that these do not have an important influence on the E_T flow.

The new measurements are shown in Fig. 3. We present the E_T flow in 7 regions in x and Q^2 and compare them again to the 3 standard Monte Carlo models. The $\langle Q^2 \rangle$ covers a range from 175 GeV^2 to 2 200 GeV^2, $\langle x \rangle$ a range from 0.0043 to 0.11. For the sake of consistency with the low Q^2 results the E_{fwd} cut is applied although its influence is small at high Q^2.

In the lowest Q^2 bin all MC models give similar predictions and describe well the energy flow. As Q^2 increases the models begin to differ and ARIADNE especially falls below the data. LEPTO slightly overshoots the E_T in all bins but describes the shape and its Q^2 and x dependence well. HERWIG follows the data closely in all but the highest $\langle W \rangle$ bins (see also Fig. 5).

4.3 Dependence on Q^2 and W

As described in the introduction electron-proton scattering can be understood as a hadron-hadron process. The exchanged γ fluctuates into a hadronic object which then scatters off

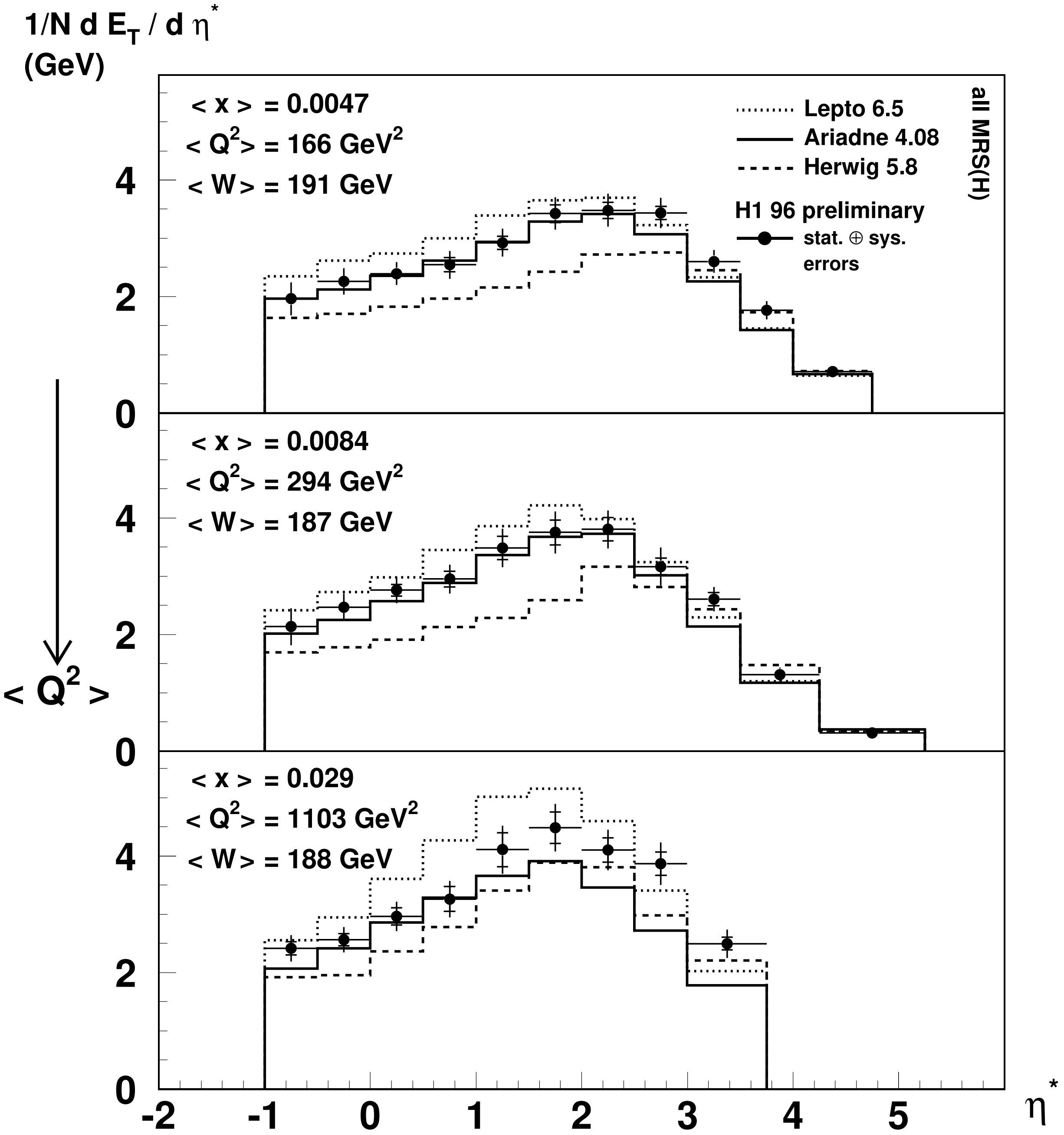

Figure 5: H1 preliminary results on the E_T flow in the hCMS at high Q^2 and $W \approx 185$ GeV. Systematic and statistical errors are added in quadrature. The data is compared to 3 MC generators: ARIADNE 4.08, HERWIG 5.8 and LEPTO 6.5. The structure functions used are based on the MRS(H) parametrizations [16].

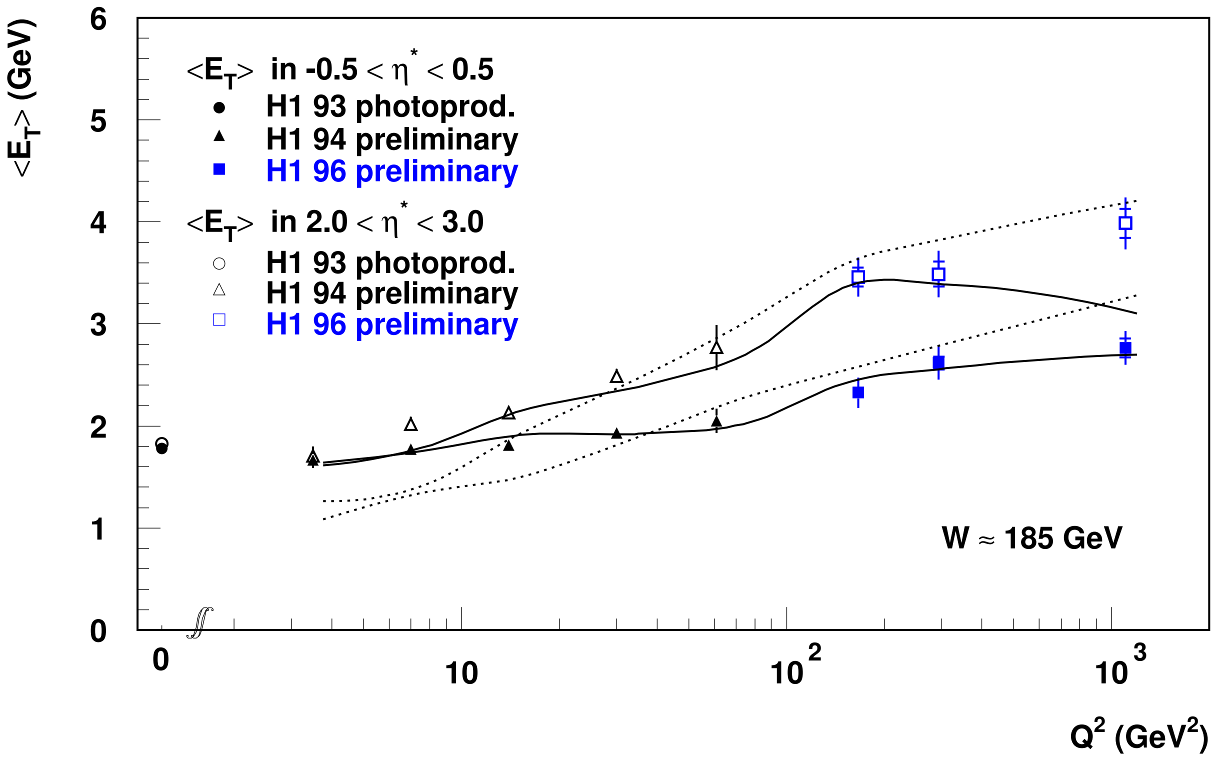

Figure 6: H1 preliminary results on the mean E_T in the central rapidity bin and the fragmentation region as a function of Q^2. 1994 data: only statistical errors included, 1996 data: statistical and systematic errors added in quadrature. Here the E_{fwd} cut is not made. Solid line: ARIADNE 4.08, dotted line: LEPTO 6.5. The structure functions used are based on the MRS(H) parametrizations [16].

the proton. In a previous publication H1 showed that this picture is not only valid in the domain of photoproduction but also in DIS [5]. From hadron-hadron data (see Fig. 4 for pp and $p\bar{p}$), the central pseudorapidity range is expected to be insensitive to the structure of the colliding particles, which, for the virtual photon in DIS, is governed by Q^2 [2]. In this region a similar level of $\langle E_T \rangle$ and a W dependence similar to hadron-hadron collisions was reported in our earlier publication. This is also true for the new analysis presented here although the improved statistics allow us to build a more precise picture of the Q^2 dependence.

Fig. 4 shows the W dependence of the new H1 high Q^2 data[4] in the central rapidity region ($|\eta^*| < 0.5$) together with our published low Q^2 results and hadron-hadron data. Again we find a similar W dependence compared to the hadron-hadron data but the mean transverse energy is clearly larger at high Q^2. For a given Q^2 the increase is in agreement with a linear dependence on $\ln W$.

In order to investigate the Q^2 dependence separately we have selected data from a small range in W (165 GeV $< W <$ 213 GeV). Since the physical picture of an hadronic fluctuation does not distinguish between rapidity gap and non-rapidity gap events the E_{fwd} cut is removed for this part of the analysis. These *fixed-W* transverse energy flow measurements are shown in Fig. 5 for the high Q^2 sample together with predictions of the 3 standard Monte Carlo models.

[4] The 96 data points in Fig. 4 are taken from Fig. 3. Therefore the E_{fwd} cut is applied but at these high Q^2 values the difference is negligible.

In Fig. 6 $\langle E_T \rangle$ is presented for two slices in η^*, the *central bin* $(-0.5 < \eta^* < 0.5)$ and the so-called *fragmentation bin* $(2 < \eta^* < 3)$ together for the low and the high Q^2 sample. The definition of the *fragmentation bin* is somewhat arbitrarily. The chosen region in η^* is expected to be dominated by the fragmentation of the hadronic fluctuation of the photon.

The transverse energy in the *fragmentation bin* and in the *central bin* are seen to rise with Q^2. Qualitatively the increase in the photon fragmentation region is consistent with e.g. the Generalized Vector Dominance Model [18], in which mesons with higher masses, and therefore higher intrinsic p_T, can contribute to the scattering at higher Q^2. In a more formal approach [19] one can demonstrate that the photon wave function allows for $q\bar{q}$ states with higher p_T at higher Q^2. However, the influence of the photon virtuality on the E_T flow in the central region was not expected and is observed here for the first time. The Q^2 independence of the *central bin* clearly breaks down although x is still of the order of 10^{-2}, even at the highest Q^2 bin.

The main features of our data can be understood assuming a photon fragmentation region of width $\sim \ln Q^2/m^2$, where m is a typical hadron mass. Since the rapidity is limited to $\pm \ln W/m$ the photon fragmentation region starts to overlap with the central rapidity region of the hCMS as Q^2 increases. If we approximate rapidity by pseudorapidity this can be seen in Fig. 5. The maximum of the E_T flow does not only increase with Q^2 but also its position moves towards the central pseudorapidity region. This also explains partly the pattern of increase (Fig. 6) observed in the *fragmentation bin*. After an approximately linear increase below $Q^2 \approx 100$ GeV^2 there is a stronger rise and then again a slower increase. The slower increase at high Q^2 is related to our definition of the *fragmentation bin* as can be seen in Fig. 5. The position of the maximum moves out of the rapidity interval of the *fragmentation bin* thereby reducing the amount of transverse energy observed in this interval.

The comparison with ARIADNE and LEPTO shows that a pQCD based Monte Carlo can describe the increase. However, none of these models satisfactorily follow the data; LEPTO shows a steeper increase in E_T with Q^2, while ARIADNE, despite giving good description of the central rapidity bin, fails to describe the fragmentation region at the highest measured Q^2 point.

Summary

The transverse energy flow has been measured for deep-inelastic scattering events observed in positron-proton collisions at HERA. The data cover a range in Q^2 from 2.5 GeV^2 to $40\,000$ GeV^2 and Bjorken-x down to $3 \cdot 10^{-5}$. We have extended the accessible pseudorapidity region towards the proton direction down to $\eta^* \sim -3$ at low Q^2 and find a smaller transverse energy in the vicinity of the proton remnant than observed centrally.

With the precision gained from higher statistics and better understanding of systematic effects, a measurement of the transverse energy flow at high Q^2 has been performed. For high Q^2 ($Q^2 > 100$ GeV^2) an increase in $\langle E_T \rangle$ in the central rapidity region is observed which is at variance with the simple picture of the photon fluctuating into and acting as a hadron. Such an increase is not expected from hadron-hadron collisions and is observed in our data for the first time. None of the pQCD based Monte Carlo models give a perfect description of all the measurements.

Acknowledgements

We are grateful to the HERA machine group whose outstanding efforts have made and continue to make this experiment possible. We thank the engineers and technicians for their work constructing and maintaining the H1 detector, our funding agencies for financial support, the DESY technical staff for continual assistance and the DESY directorate for the hospitality which they extend to the non-DESY members of the collaboration.

References

[1] H1 Collaboration (I. Abt et al.), *Z. Phys.* C **63**, 377 (1994).

[2] J.D. Bjorken and J.B. Kogut, *Phys. Rev.* D **8**, 1341 (1973).

[3] V. Del Duca et al., *Phys. Rev.* D **46**, 931 (1992).

[4] G. Shaw, *Phys. Lett.* B **318**, 221 (1993); G. Kerley and G. Shaw, *Phys. Rev.* D **56**, 7291 (1997).

[5] H1 Collaboration (S. Aid et al.), *Phys. Lett.* B **356**, 118 (1995).

[6] M.F. Hess, *Messung des transversalen Energieflusses mit dem H1-Detektor bei HERA*, Ph.D. thesis, Hamburg 1996, MPI-PhE/96-16; D. Krücker in *Proc. of the 3rd Workshop in Small-x and Diff. Physics*, Argonne 1996.

[7] E. Penaro, Ph.D thesis, in preparation.

[8] H1 Collaboration (I.Abt et al.), *Nucl. Instrum. Methods* A **368**, 310 (1997), ibid p.386.

[9] F. Jacquet and A. Blondel in Proceedings of the Study of an ep Facility for Europe, ed. U. Amaldi, DESY 79-48, p.391 (1979).

[10] U. Bassler and G. Bernardi, DESY 94-231.

[11] G. A. Schuler and H. Spiesberger, Proceedings of the Workshop Physics at HERA, vol. 3, eds. W. Buchmüller and G. Ingelman, DESY (1992) p.1419; K. Charchula, T. Ahmed and H. Spiesberger, CERN-TH 7133/94.

[12] L. Lönnblad, Ariadne version 4.08 program and manual, *Comp. Phys. Comm.* **71**, 15 (1992).

[13] G. Marchesini et al., *Comp. Phys. Comm.* **67**, 465 (1993).

[14] G. Ingelman, A. Edin, J. Rathsman, *Comp. Phys. Comm.* **101**, 108 (1997).

[15] M. Glück, E. Reya and A. Vogt, *Z. Phys.* C **67**, 433 (1995).

[16] A.D. Martin, W.J. Stirling and R.G. Roberts, MRS Parton Distributions, Proc. of the Workshop on Quantum Field Theory Theoretical Aspects of High Energy Physics, eds. B. Geyser and E.M. Ilgenfritz, p.11, (1993).

[17] UA1 Collab., C. Albajar et al., *Nucl. Phys.* B **335**, 261 (1990); A. De Roeck, Inclusive Particle Production in Hadron-Proton Interactions at 250 GeV/c, Ph.D. Thesis, Antwerpen 1988.

[18] A. Donnachie and G. Shaw, in Electromagnetic interactions of hadrons, Vol. 2, 169-194, eds. A. Donnachie and G. Shaw, Plenum, New York (1978).

[19] S. Brodsky et al., *Phys. Rev.* D **50**, 3134 (1994), S. Brodsky and P. Lepage, *Phys. Rev.* D **22**, 2157 (1980)